

## BLIND IMAGE DEBLURRING USING JUMP REGRESSION ANALYSIS

Peihua Qiu and Yicheng Kang

*Department of Biostatistics, University of Florida*

### Supplementary Material

This supplementary file contains a description of the roof/valley edge detection procedure, proofs of the theoretical results presented in Section 3 of the paper, and some simulation results about the proposed method.

## S.1 Roof/Valley Edge Detection

In this part, we describe our proposed roof/valley edge detection procedure. The methodology is similar to the step edge detection procedure described in the paper. For any given design point  $(x, y) \in [k_2/n, 1 - k_2/n] \times [k_2/n, 1 - k_2/n]$ , where the positive integer  $k_2 < n/2$  is the bandwidth parameter for roof/valley edge detection, let us consider a circular neighborhood  $O_n''(x, y) = \{(u, v) : (u, v) \in \Omega, \sqrt{(u-x)^2 + (v-y)^2} \leq k_2/n\}$  and the following local quadratic kernel (LQK) smoothing procedure:

$$\min_{c_0, c_1, c_2, c_3, c_4, c_5 \in \mathbb{R}} \sum_{i^2 + j^2 \leq k_2^2} \left\{ Z(x + i/n, y + j/n) - \left[ c_0 + c_1 \frac{i}{n} + c_2 \frac{j}{n} + \frac{c_3}{2} \left( \frac{i}{n} \right)^2 + \frac{c_4}{2} \left( \frac{j}{n} \right)^2 + c_5 \frac{ij}{n^2} \right] \right\}^2 K^* \left( \frac{i}{k_2}, \frac{j}{k_2} \right). \quad (\text{S.1})$$

Let  $(\hat{c}_0(x, y), \hat{c}_1(x, y), \hat{c}_2(x, y), \hat{c}_3(x, y), \hat{c}_4(x, y), \hat{c}_5(x, y))$  denote the solution to  $(c_0, c_1, c_2, c_3, c_4, c_5)$  of (S.1). Then,  $\hat{c}_3(x, y)$  and  $\hat{c}_4(x, y)$  are LQK estimators of  $f''_{xx}(x, y)$  and  $f''_{yy}(x, y)$ . Similar to step edge detection, we divide  $O_n''(x, y)$  into two halves, denoted as  $U_n''(x, y)$  and  $V_n''(x, y)$ , along the direction perpendicular to  $(\hat{c}_3(x, y), \hat{c}_4(x, y))$ . To detect jumps in  $f'_x$ , we define

$$M_{1,n}^{(2)}(x, y) = \frac{|\hat{b}_+(x, y) - \hat{b}_-(x, y)|}{\sqrt{\frac{\sum_{U_n''(x,y)} g_{ij}(x,y)^2}{[\sum_{U_n''(x,y)} g_{ij}(x,y)]^2} + \frac{\sum_{V_n''(x,y)} g'_{ij}(x,y)^2}{[\sum_{V_n''(x,y)} g'_{ij}(x,y)]^2}}},$$

where  $\widehat{b}_+(x, y)$  and  $\widehat{b}_-(x, y)$  are respectively the solutions to  $b$  of the following local weighted least square problems:

$$\min_{a,b,c} \sum_{U_n''(x,y)} [Z(x + \frac{i}{n}, y + \frac{j}{n}) - (a + b\frac{i}{n} + c\frac{j}{n})]^2 K^* \left( \frac{i}{k_2}, \frac{j}{k_2} \right) L^* \left( \frac{d_{ij}''}{k_2/n} \right), \quad (\text{S.2})$$

$$\min_{a,b,c} \sum_{V_n''(x,y)} [Z(x + \frac{i}{n}, y + \frac{j}{n}) - (a + b\frac{i}{n} + c\frac{j}{n})]^2 K^* \left( \frac{i}{k_2}, \frac{j}{k_2} \right) L^* \left( \frac{d_{ij}''}{k_2/n} \right), \quad (\text{S.3})$$

$$\begin{aligned} g_{ij}(x, y) &= [G_1(x, y) + G_2(x, y)\frac{i}{n} + G_3(x, y)\frac{j}{n}] K^* \left( \frac{i}{k_2}, \frac{j}{k_2} \right) L^* \left( \frac{d_{ij}''}{k_2/n} \right), \\ G_1(x, y) &= u_{11}(x, y)u_{01}(x, y) - u_{10}(x, y)u_{02}(x, y), \\ G_2(x, y) &= u_{00}(x, y)u_{02}(x, y) - u_{01}(x, y)u_{01}(x, y), \\ G_3(x, y) &= u_{01}(x, y)u_{10}(x, y) - u_{00}(x, y)u_{11}(x, y), \\ u_{s_1, s_2}(x, y) &= \sum_{U_n''(x,y)} \left( \frac{i}{n} \right)^{s_1} \left( \frac{j}{n} \right)^{s_2} K^* \left( \frac{i}{k_2}, \frac{j}{k_2} \right) L^* \left( \frac{d_{ij}''}{k_2/n} \right), \quad s_1, s_2 = 0, 1, 2, \end{aligned}$$

$g'_{ij}(x, y)$  is defined in the same way as  $g_{ij}(x, y)$ , except that  $U_n''(x, y)$  in the definition of  $u_{s_1, s_2}(x, y)$  should be replaced by  $V_n''(x, y)$ , and  $d_{ij}''$  is the Euclidean distance from the design point  $(x_i, y_j)$  to the line separating  $U_n''(x, y)$  from  $V_n''(x, y)$ . Similarly, to detect jumps in  $f'_y$ , we define

$$M_{2,n}^{(2)}(x, y) = \frac{|\widehat{c}_+(x, y) - \widehat{c}_-(x, y)|}{\sqrt{\frac{\sum_{U_n''(x,y)} h_{ij}(x,y)^2}{[\sum_{U_n''(x,y)} h_{ij}(x,y)]^2} + \frac{\sum_{V_n''(x,y)} h'_{ij}(x,y)^2}{[\sum_{V_n''(x,y)} h'_{ij}(x,y)]^2}}},$$

where  $\widehat{c}_+(x, y)$  and  $\widehat{c}_-(x, y)$  are respectively the solutions to  $c$  of (S.2) and (S.3),

$$\begin{aligned} h_{ij}(x, y) &= [H_1(x, y) + H_2(x, y)\frac{i}{n} + H_3(x, y)\frac{j}{n}] K^* \left( \frac{i}{k_2}, \frac{j}{k_2} \right) L^* \left( \frac{d_{ij}''}{k_2/n} \right), \\ H_1(x, y) &= u_{10}(x, y)u_{11}(x, y) - u_{01}(x, y)u_{20}(x, y), \\ H_2(x, y) &= u_{01}(x, y)u_{10}(x, y) - u_{00}(x, y)u_{11}(x, y), \\ H_3(x, y) &= u_{00}(x, y)u_{20}(x, y) - u_{10}(x, y)u_{10}(x, y), \end{aligned}$$

and  $h'_{ij}(x, y)$  is defined in the same way as  $h_{ij}(x, y)$ , except that  $U_n''(x, y)$  in the definition of  $u_{s_1, s_2}(x, y)$  should be replaced by  $V_n''(x, y)$ . Then, the design point  $(x, y)$  is flagged as a roof/valley edge pixel if

$$M_n^{(2)}(x, y) = \max \{ M_{1,n}^{(2)}(x, y), M_{2,n}^{(2)}(x, y) \} > v_n \sigma,$$

where  $v_n$  is a threshold value. However, this criterion could be large around step edges too, due to the zero-crossing properties of the second-order derivatives around step edges (cf., Qiu 2005, Figure 6.2). To overcome this difficulty, we propose flagging  $(x, y)$  as a roof/valley edge pixel if

$$I_n(x, y) = 0, \text{ and } M_n^{(2)}(x, y) > v_n \sigma, \quad (\text{S.4})$$

where  $I_n(x, y)$  denotes the number of detected step edge pixels in  $O_n''(x, y)$ . The two modification procedures in Qiu and Yandell (1997) can also be used here to remove the two types of deceptive roof/valley edge pixels detected by (S.4). Again,  $\sigma$  should be replaced by  $\hat{\sigma}$  in practice.

## S.2 Proofs of Theorems 3.1 and 3.2

**Lemma 1.** *Under the conditions of Theorem 3.1, the estimated gradient  $(\hat{b}(x, y), \hat{c}(x, y))$  obtained from the local linear kernel smoothing procedure (3) in the paper has the following properties:*

(i) *If  $f$  has continuous first order derivatives at  $(x, y)$ , then*

$$(\hat{b}(x, y), \hat{c}(x, y)) \rightarrow (f'_x(x, y), f'_y(x, y)), \text{ a.s.,} \quad \text{as } n \rightarrow \infty. \quad (\text{S.5})$$

(ii) *If  $(x, y)$  is a nonsingular point on a roof/valley edge, i.e.,  $f$  is continuous at  $(x, y)$  and has finite first order directional derivatives but the limits of  $f'_x$  or  $f'_y$  from the two parts separated by the roof/valley edge are not the same, then*

$$\begin{aligned} (\hat{b}(x, y), \hat{c}(x, y)) &\rightarrow \frac{1}{2} (f'_{x+}(x, y) + f'_{x-}(x, y), \\ &f'_{y+}(x, y) + f'_{y-}(x, y)), \text{ a.s., as } n \rightarrow \infty, \end{aligned} \quad (\text{S.6})$$

where  $f'_{x+}(x, y)$ ,  $f'_{x-}(x, y)$ ,  $f'_{y+}(x, y)$ , and  $f'_{y-}(x, y)$  denote the limits of the first order derivatives of  $f(u, v)$  as  $(u, v)$  approaches  $(x, y)$  from the two parts separated by the roof/valley edge.

(iii) *If  $(x, y)$  is a nonsingular point on a step edge which has a tangent line at  $(x, y)$ , then*

$$\frac{(\hat{b}(x, y), \hat{c}(x, y))}{\sqrt{\hat{b}(x, y)^2 + \hat{c}(x, y)^2}} \rightarrow (-\sin \theta, \cos \theta), \text{ a.s.,} \quad \text{as } n \rightarrow \infty, \quad (\text{S.7})$$

where  $\theta$  is the angle formed by the tangent line of the JLC at  $(x, y)$  and the  $x$ -axis.

**Proof** Recall that  $(x_i, y_j) = (i/n, j/n)$ , for  $i, j = 1, 2, \dots, n$ , and  $R_n = \sup_{i,j} r_n(i/n, j/n)$ , where  $r_n(i/n, j/n)$  is the blurring extent at  $(i/n, j/n)$ . Then, it is not difficult to verify that the solution of (3) in the paper has the expressions

$$\begin{aligned} \hat{b}(x, y) &= \frac{1}{r_{20}^*} \sum_{i^2+j^2 \leq k_1^2} \frac{i}{n} Z \left( x + \frac{i}{n}, y + \frac{j}{n} \right) K^* \left( \frac{i}{k_1}, \frac{j}{k_1} \right), \\ \hat{c}(x, y) &= \frac{1}{r_{02}^*} \sum_{i^2+j^2 \leq k_1^2} \frac{j}{n} Z \left( x + \frac{i}{n}, y + \frac{j}{n} \right) K^* \left( \frac{i}{k_1}, \frac{j}{k_1} \right), \end{aligned}$$

where  $r_{s_1 s_2}^* = \sum_{i^2+j^2 \leq k_1^2} \left(\frac{i}{n}\right)^{s_1} \left(\frac{j}{n}\right)^{s_2} K^* \left(\frac{i}{k_1}, \frac{j}{k_1}\right)$ , for  $s_1, s_2 = 0, 1, 2$ . To prove the result (S.5), we notice that if  $f$  has continuous derivatives at  $(x, y)$ , then

$$\mathbb{E}(\widehat{b}(x, y)) = \frac{1}{r_{20}^*} \sum_{i^2+j^2 \leq k_1^2} H\{f\} \left(x + \frac{i}{n}, y + \frac{j}{n}\right) \frac{i}{n} K^* \left(\frac{i}{k_1}, \frac{j}{k_1}\right), \quad (\text{S.8})$$

where

$$\begin{aligned} H\{f\}(\xi_i, \gamma_j) &= \int \int_{u^2+v^2 \leq \left(\frac{r_n(\xi_i, \gamma_j)}{n}\right)^2} h(u, v; \xi_i, \gamma_j) f(\xi_i - u, \gamma_j - v) \, dudv \\ &= \int \int_{u^2+v^2 \leq \left(\frac{r_n(\xi_i, \gamma_j)}{n}\right)^2} h(u, v; \xi_i, \gamma_j) [f(\xi_i, \gamma_j) - f'_x(\xi_i, \gamma_j)u \\ &\quad - f'_y(\xi_i, \gamma_j)v + o\left(\frac{r_n(\xi_i, \gamma_j)}{n}\right)] \, dudv \\ &= f(\xi_i, \gamma_j) + O(R_n/n), \end{aligned} \quad (\text{S.9})$$

and  $(\xi_i, \gamma_j) = \left(x + \frac{i}{n}, y + \frac{j}{n}\right)$ . By (S.8) and (S.9), we have

$$\begin{aligned} &\mathbb{E}(\widehat{b}(x, y)) \\ &= \frac{1}{r_{20}^*} \sum_{i^2+j^2 \leq k_1^2} [f(x + i/n, y + j/n) + O(R_n/n)] \frac{i}{n} K^* \left(\frac{i}{k_1}, \frac{j}{k_1}\right) \\ &= \frac{1}{r_{20}^*} \sum_{i^2+j^2 \leq k_1^2} [f(x, y) + f'_x(x, y)i/n + f'_y(x, y)j/n + O(k_1^2/n^2)] \frac{i}{n} K^* \left(\frac{i}{k_1}, \frac{j}{k_1}\right) \\ &\quad + \frac{1}{r_{20}^*} \sum_{i^2+j^2 \leq k_1^2} O(R_n/n) \frac{i}{n} K^* \left(\frac{i}{k_1}, \frac{j}{k_1}\right) \\ &= \frac{f(x, y)}{r_{20}^*} \sum_{i^2+j^2 \leq k_1^2} \frac{i}{n} K^* \left(\frac{i}{k_1}, \frac{j}{k_1}\right) + f'_x(x, y) + \\ &\quad \frac{f'_y(x, y)}{r_{20}^*} \sum_{i^2+j^2 \leq k_1^2} \frac{ij}{n^2} K^* \left(\frac{i}{k_1}, \frac{j}{k_1}\right) + \frac{O(R_n/n) + O(k_1^2/n^2)}{k_1/n} \\ &= f'_x(x, y) + O(R_n/k_1) + O(k_1/n). \end{aligned}$$

In the last equation of the above expression, we have used the results that  $\sum_{i^2+j^2 \leq k_1^2} \frac{i}{n} K^* \left(\frac{i}{k_1}, \frac{j}{k_1}\right) = 0$ ,  $\sum_{i^2+j^2 \leq k_1^2} \frac{ij}{n^2} K^* \left(\frac{i}{k_1}, \frac{j}{k_1}\right) = 0$ , by the circular symmetry of  $K^*$ . We have also used the result that  $r_{20}^* = O(k_1^4/n^2)$ , which can be proved similarly to expression (23) in Proposition 2 of Qiu (2009). Then by (24) in Proposition 2 of Qiu (2009), we have

$$\frac{1}{k_1^2} \sum_{i^2+j^2 \leq k_1^2} \varepsilon_{ij} \phi \left(\frac{i}{k_1}, \frac{j}{k_1}\right) K^* \left(\frac{i}{k_1}, \frac{j}{k_1}\right) = O\left(\frac{\log n}{k_1}\right), \quad a.s., \quad (\text{S.10})$$

where  $\phi(u, v)$  is any Lipschitz-1 continuous function defined in the region  $\{(u, v) : u^2 + v^2 \leq 1\}$ . By (S.8) and the fact that  $r_{20}^* = O(k_1^4/n^2)$ , we have

$$\widehat{b}(x, y) - \mathbb{E}(\widehat{b}(x, y)) = \frac{1}{r_{20}^*} \sum_{i^2+j^2 \leq k_1^2} \varepsilon_{ij} \frac{i}{n} K^* \left(\frac{i}{k_1}, \frac{j}{k_1}\right) = O\left(\frac{n \log(n)}{k_1^2}\right), \quad a.s. \quad (\text{S.11})$$

Similarly, we have

$$\widehat{c}(x, y) - \mathbb{E}(\widehat{c}(x, y)) = \frac{1}{r_{02}^*} \sum_{i^2+j^2 \leq k_1^2} \varepsilon_{ij} \frac{j}{n} K^* \left( \frac{i}{k_1}, \frac{j}{k_1} \right) = O \left( \frac{n \log(n)}{k_1^2} \right), \text{ a.s.} \quad (\text{S.12})$$

After combining (S.11) and (S.12), (S.5) is proved.

Now, assume that  $(x, y)$  is a nonsingular point on a roof/valley edge segment. Since  $f$  has bounded directional first-order derivatives, we can find a positive constant  $C$  such that for any two points  $(x_i, y_j)$  and  $(x_i - u, y_j - v)$  in a neighborhood of  $(x, y)$ , we have

$$f(x_i, y_j) - C\sqrt{u^2 + v^2} \leq f(x_i - u, y_j - v) \leq f(x_i, y_j) + C\sqrt{u^2 + v^2}.$$

Consequently,  $f(x_i, y_j) - C \frac{r_n(x_i, y_j)}{n} \leq \int \int_{u^2+v^2 \leq (\frac{r(x_i, y_j)}{n})^2} h(u, v; x_i, y_j) f(x_i - u, y_j - v) dudv \leq f(x_i, y_j) + C \frac{r_n(x_i, y_j)}{n}$ . So,

$$H\{f\}(x_i, y_j) = f(x_i, y_j) + O(r_n(x_i, y_j)/n). \quad (\text{S.13})$$

Because  $(x, y)$  is a nonsingular point, the related roof/valley edge segment has a unique tangent line at  $(x, y)$ . Without loss of generality, let us assume that (i) the roof/valley edge segment in  $O'_n(x, y)$  is a straight line, which forms an angle  $\theta$  with the  $x$ -axis, and (ii) the roof/valley edge segment divides  $O'_n(x, y)$  into two parts  $O'_{1n}(x, y)$  and  $O'_{2n}(x, y)$ , where  $O'_{1n}(x, y)$  contains the upper-right quarter of  $O'_n(x, y)$  and  $O'_{2n}(x, y)$  contains the lower-left quarter of  $O'_n(x, y)$ . The first assumption is reasonable because the difference between the roof/valley edge segment and the tangent line at  $(x, y)$  is negligible in  $O'_n(x, y)$  when  $n$  is sufficiently large. Then, we have

$$\begin{aligned} & \mathbb{E}(\widehat{b}(x, y)) \\ &= \frac{1}{r_{20}^*} \left( \sum_{O'_{1n}(x, y)} + \sum_{O'_{2n}(x, y)} \right) [f(x + i/n, y + j/n) + O(R_n/n)] \frac{i}{n} K^* \left( \frac{i}{k_1}, \frac{j}{k_1} \right) \\ &= \frac{1}{r_{20}^*} \sum_{O'_{1n}(x, y)} \left[ f(x, y) + f'_{x+}(x, y) \frac{i}{n} + f'_{y+}(x, y) \frac{j}{n} \right] \frac{i}{n} K^* \left( \frac{i}{k_1}, \frac{j}{k_1} \right) + \\ & \quad \frac{1}{r_{20}^*} \sum_{O'_{2n}(x, y)} \left[ f(x, y) + f'_{x-}(x, y) \frac{i}{n} + f'_{y-}(x, y) \frac{j}{n} \right] \frac{i}{n} K^* \left( \frac{i}{k_1}, \frac{j}{k_1} \right) + \\ & \quad \frac{1}{r_{20}^*} \sum_{O'_n(x, y)} [O(R_n/n) + O(k_1^2/n^2)] \frac{i}{n} K^* \left( \frac{i}{k_1}, \frac{j}{k_1} \right) \\ &= \frac{f(x, y)}{r_{20}^*} \sum_{O'_n(x, y)} \frac{i}{n} K^* \left( \frac{i}{k_1}, \frac{j}{k_1} \right) + \frac{f'_{x+}(x, y)}{r_{20}^*} \sum_{O'_{1n}(x, y)} \left( \frac{i}{n} \right)^2 K^* \left( \frac{i}{k_1}, \frac{j}{k_1} \right) + \\ & \quad \frac{f'_{x-}(x, y)}{r_{20}^*} \sum_{O'_{2n}(x, y)} \left( \frac{i}{n} \right)^2 K^* \left( \frac{i}{k_1}, \frac{j}{k_1} \right) + \frac{f'_{y+}(x, y)}{r_{20}^*} \sum_{O'_{1n}(x, y)} \frac{i}{n} \frac{j}{n} K^* \left( \frac{i}{k_1}, \frac{j}{k_1} \right) \\ & + \frac{f'_{y-}(x, y)}{r_{20}^*} \sum_{O'_{2n}(x, y)} \frac{i}{n} \frac{j}{n} K^* \left( \frac{i}{k_1}, \frac{j}{k_1} \right) + O(R_n/k_1) + O(k_1/n) \end{aligned}$$

$$\begin{aligned}
&= \left( \frac{f'_{x+}(x,y)}{r_{20}^*} \sum_{O'_{1n}(x,y)} + \frac{f'_{x-}(x,y)}{r_{20}^*} \sum_{O'_{2n}(x,y)} \right) \left( \frac{i}{n} \right)^2 K^* \left( \frac{i}{k_1}, \frac{j}{k_1} \right) + \\
&\quad \left( \frac{f'_{y+}(x,y)}{r_{20}^*} \sum_{O'_{1n}(x,y)} + \frac{f'_{y-}(x,y)}{r_{20}^*} \sum_{O'_{2n}(x,y)} \right) \frac{i}{n} \frac{j}{n} K^* \left( \frac{i}{k_1}, \frac{j}{k_1} \right) \\
&\quad + O(R_n/k_1) + O(k_1/n),
\end{aligned}$$

where we have used the result that  $r_{10}^* = 0$  due to the circular symmetry of  $K^*$ . Also observe the following facts:

$$\begin{aligned}
\frac{\sum_{O'_{1n}(x,y)} (i/n)^2 K^* \left( \frac{i}{k_1}, \frac{j}{k_1} \right)}{r_{20}^*} &= \frac{\int_{\theta}^{\theta+\pi} d\varphi \int_0^1 r^3 \cos^2 \varphi \tilde{K}^*(r) dr}{\int_0^{2\pi} d\varphi \int_0^1 r^3 \cos^2 \varphi \tilde{K}^*(r) dr} + O(1/k_1) \\
&= \frac{1}{2} + O(1/k_1), \\
\frac{\sum_{O'_{2n}(x,y)} (i/n)^2 K^* \left( \frac{i}{k_1}, \frac{j}{k_1} \right)}{r_{20}^*} &= \frac{\int_{\theta+\pi}^{\theta+2\pi} d\varphi \int_0^1 r^3 \cos^2 \varphi \tilde{K}^*(r) dr}{\int_0^{2\pi} d\varphi \int_0^1 r^3 \cos^2 \varphi \tilde{K}^*(r) dr} + O(1/k_1) \\
&= \frac{1}{2} + O(1/k_1), \\
\frac{\sum_{O'_{1n}(x,y)} (i/n)(j/n) K^* \left( \frac{i}{k_1}, \frac{j}{k_1} \right)}{r_{20}^*} &= \frac{\int_{\theta}^{\theta+\pi} d\varphi \int_0^1 r^3 \cos \varphi \sin \varphi \tilde{K}^*(r) dr}{\int_0^{2\pi} d\varphi \int_0^1 r^3 \cos^2 \varphi \tilde{K}^*(r) dr} + O(1/k_1) \\
&= 0 + O(1/k_1), \\
\frac{\sum_{O'_{2n}(x,y)} (i/n)(j/n) K^* \left( \frac{i}{k_1}, \frac{j}{k_1} \right)}{r_{20}^*} &= \frac{\int_{\theta+\pi}^{\theta+2\pi} d\varphi \int_0^1 r^3 \cos \varphi \sin \varphi \tilde{K}^*(r) dr}{\int_0^{2\pi} d\varphi \int_0^1 r^3 \cos^2 \varphi \tilde{K}^*(r) dr} + O(1/k_1) \\
&= 0 + O(1/k_1),
\end{aligned}$$

where  $\tilde{K}^*(r) = K^*(r \cos \varphi, r \sin \varphi)$ . Then we have

$$E(\hat{b}(x,y)) = \frac{f'_{x-}(x,y) + f'_{x+}(x,y)}{2} + O(1/k_1) + O(R_n/k_1) + O(k_1/n). \quad (\text{S.14})$$

By (S.11) and (S.14), we have

$$\hat{b}(x,y) = \frac{f'_{x-}(x,y) + f'_{x+}(x,y)}{2} + O(1/k_1) + O(R_n/k_1) + O(k_1/n) + O\left(\frac{n \log n}{k_1^2}\right).$$

Similarly, we have

$$\hat{c}(x,y) = \frac{f'_{y-}(x,y) + f'_{y+}(x,y)}{2} + O(1/k_1) + O(R_n/k_1) + O(k_1/n) + O\left(\frac{n \log n}{k_1^2}\right).$$

Then, (S.6) is proved.

Now, if  $(x,y)$  is a nonsingular point on a step edge segment, then  $O'_n(x,y)$  consists of the following three disjoint parts  $O'_{n,l}(x,y)$ ,  $O'_{n,c}(x,y)$ , and  $O'_{n,r}(x,y)$ , where  $O'_{n,c}(x,y)$  is a band of width  $2R_n/n$  containing a step edge segment in its middle, and  $O'_{n,l}(x,y)$  and  $O'_{n,r}(x,y)$  are on its two different sides. Since  $(x,y)$  is nonsingular, the step edge segment has a unique tangent line at  $(x,y)$ . Also, without loss of generality, we can assume that the step edge segment is a straight line in  $O'_n(x,y)$  and it forms an angle  $\theta$

with the  $x$ -axis. Then, we have

$$\begin{aligned}
& \mathbb{E}(\widehat{b}(x, y)) \tag{S.15} \\
&= \frac{1}{r_{20}^*} \left( \sum_{O'_{n,l}(x,y)} + \sum_{O'_{n,c}(x,y)} + \sum_{O'_{n,r}(x,y)} \right) H\{f\} \left( x + \frac{i}{n}, y + \frac{j}{n} \right) \frac{i}{n} K^* \left( \frac{i}{k_1}, \frac{j}{k_1} \right) \\
&= \frac{1}{r_{20}^*} \sum_{O'_{n,l}(x,y)} \left[ f \left( x + \frac{i}{n}, y + \frac{j}{n} \right) + O \left( \frac{R_n}{n} \right) \right] \frac{i}{n} K^* \left( \frac{i}{k_1}, \frac{j}{k_1} \right) + \\
&\quad \frac{1}{r_{20}^*} \sum_{O'_{n,c}(x,y)} H\{f\} \left( x + \frac{i}{n}, y + \frac{j}{n} \right) \frac{i}{n} K^* \left( \frac{i}{k_1}, \frac{j}{k_1} \right) + \\
&\quad \frac{1}{r_{20}^*} \sum_{O'_{n,r}(x,y)} \left[ f \left( x + \frac{i}{n}, y + \frac{j}{n} \right) + O \left( \frac{R_n}{n} \right) \right] \frac{i}{n} K^* \left( \frac{i}{k_1}, \frac{j}{k_1} \right) \\
&= \frac{1}{r_{20}^*} \sum_{O'_{n,l}(x,y)} \left[ f_-(x, y) + O(k_1/n) + O(R_n/n) \right] \frac{i}{n} K^* \left( \frac{i}{k_1}, \frac{j}{k_1} \right) + O \left( \frac{nR_n}{k_1^2} \right) \\
&+ \frac{1}{r_{20}^*} \sum_{O'_{n,r}(x,y)} \left[ f_+(x, y) + O(k_1/n) + O(R_n/n) \right] \frac{i}{n} K^* \left( \frac{i}{k_1}, \frac{j}{k_1} \right) \\
&= \frac{1}{r_{20}^*} f_-(x, y) \sum_{i=1}^n \sum_{j=1}^n \frac{i}{n} K^* \left( \frac{i}{k_1}, \frac{j}{k_1} \right) - \frac{1}{r_{20}^*} f_-(x, y) \sum_{O'_{n,r}(x,y)} \frac{i}{n} K^* \left( \frac{i}{k_1}, \frac{j}{k_1} \right) \\
&- \frac{1}{r_{20}^*} f_-(x, y) \sum_{O'_{n,c}(x,y)} \frac{i}{n} K^* \left( \frac{i}{k_1}, \frac{j}{k_1} \right) + \frac{1}{r_{20}^*} f_+(x, y) \sum_{O'_{n,r}(x,y)} \frac{i}{n} K^* \left( \frac{i}{k_1}, \frac{j}{k_1} \right) \\
&+ O(R_n/k_1) + O(1) + O \left( \frac{nR_n}{k_1^2} \right) \\
&= \frac{f_+(x, y) - f_-(x, y)}{r_{20}^*} \sum_{O'_{n,r}(x,y)} \frac{i}{n} K^* \left( \frac{i}{k_1}, \frac{j}{k_1} \right) + O(1) + O \left( \frac{nR_n}{k_1^2} \right).
\end{aligned}$$

In the third equation of (S.15), we have used the results that  $r_{20}^* = O(k_1^4/n^2)$ ,  $H\{f\}(x_i, y_j)$  are uniformly bounded when  $(x_i, y_j) \in O'_{n,c}(x, y)$ , and the fact that the ratio of the area of  $O'_{n,c}(x, y)$  to the area of  $O'_n(x, y)$  is of order  $O(R_n/k_1)$ . In the fourth equation, we have used the results that  $\sum_{O'_{n,r}(x,y)} \frac{i}{n} K^* \left( \frac{i}{k_1}, \frac{j}{k_1} \right) = O(k_1^3/n)$ ,  $\sum_{O'_{n,l}(x,y)} \frac{i}{n} K^* \left( \frac{i}{k_1}, \frac{j}{k_1} \right) = O(k_1^3/n)$ , and  $r_{20}^* = O(k_1^4/n^2)$ . In the last equation, we have used the result  $r_{10}^* = 0$  and  $\frac{1}{r_{20}^*} \sum_{O'_{n,c}(x,y)} \frac{i}{n} K^* \left( \frac{i}{k_1}, \frac{j}{k_1} \right) = O \left( \frac{nR_n}{k_1^2} \right)$ . By (S.11), we have

$$\widehat{b}(x, y) = \frac{f_+(x, y) - f_-(x, y)}{r_{20}^*} \sum_{O'_{n,r}(x,y)} \frac{i}{n} K^* \left( \frac{i}{k_1}, \frac{j}{k_1} \right) + O(1) + O \left( \frac{nR_n}{k_1^2} \right) + O \left( \frac{n \log(n)}{k_1^2} \right), \text{ a.s.}$$

Similarly, we have

$$\widehat{c}(x, y) = \frac{f_+(x, y) - f_-(x, y)}{r_{02}^*} \sum_{O'_{n,r}(x,y)} \frac{j}{n} K^* \left( \frac{i}{k_1}, \frac{j}{k_1} \right) + O(1) + O \left( \frac{nR_n}{k_1^2} \right) + O \left( \frac{n \log(n)}{k_1^2} \right), \text{ a.s.}$$

By using the following two facts:

$$\frac{k_1/n}{r_{20}^*} \sum_{O'_{n,r}(x,y)} \frac{i}{n} K^* \left( \frac{i}{k_1}, \frac{j}{k_1} \right) \rightarrow \frac{\int_{\theta}^{\theta+\pi} d\varphi \int_0^1 r^2 \cos \varphi \tilde{K}^*(r) dr}{\int_0^{2\pi} d\varphi \int_0^1 r^3 \cos^2 \varphi \tilde{K}^*(r) dr} = \frac{-2 \int_0^1 r^2 \tilde{K}^*(r) dr}{\pi \int_0^1 r^3 \tilde{K}^*(r) dr} \sin \theta,$$

$$\frac{k_1/n}{r_{02}^*} \sum_{O'_{n,r}(x,y)} \frac{j}{n} \tilde{K}^* \left( \frac{i}{k_1}, \frac{j}{k_1} \right) \rightarrow \frac{\int_{\theta}^{\theta+\pi} d\varphi \int_0^1 r^2 \sin \varphi \tilde{K}^*(r) dr}{\int_0^{2\pi} d\varphi \int_0^1 r^3 \sin^2 \varphi \tilde{K}^*(r) dr} = \frac{2 \int_0^1 r^2 \tilde{K}^*(r) dr}{\pi \int_0^1 r^3 \tilde{K}^*(r) dr} \cos \theta,$$

we have,

$$\begin{aligned} \frac{(\hat{b}(x,y), \hat{c}(x,y))}{\sqrt{\hat{b}(x,y)^2 + \hat{c}(x,y)^2}} &= \frac{((k_1/n)\hat{b}(x,y), (k_1/n)\hat{c}(x,y))}{\sqrt{(k_1/n)^2 \hat{b}(x,y)^2 + (k_1/n)^2 \hat{c}(x,y)^2}} \\ &\rightarrow (-\sin \theta, \cos \theta), \text{ a.s.} \end{aligned}$$

which completes the proof of (S.7).

### Proof Of Theorem 3.1

By some routine algebraic manipulations, the solution to  $a$  in the local linear kernel smoothing problem (4) has the expression

$$\begin{aligned} \hat{a}_+(x,y) &= \frac{\sum_{U'_n(x,y)} b_{ij}(x,y) Z_{ij}}{\sum_{U'_n(x,y)} b_{ij}(x,y)} \\ &= \frac{\sum_{U'_n(x,y)} b_{ij}(x,y) H\{f\}(x_i, y_j)}{\sum_{U'_n(x,y)} b_{ij}(x,y)} + \frac{\sum_{U'_n(x,y)} b_{ij}(x,y) \varepsilon_{ij}}{\sum_{U'_n(x,y)} b_{ij}(x,y)} \\ &=: I_1(x,y) + I_2(x,y). \end{aligned} \tag{S.16}$$

Let  $\tilde{U}'_n(x,y)$  denote the half of  $O'_n(x,y)$  separated by a line passing  $(x,y)$  in the direction perpendicular to the asymptotic direction of  $(\hat{b}(x,y), \hat{c}(x,y))$ , which is given in Lemma 1, and  $\tilde{d}'_{ij}$  denote the Euclidean distance from  $(x_i, y_j)$  to that dividing line. For a function  $\phi$  satisfying the condition that  $\sup_{u^2+v^2 \leq 1} |\phi(u,v)| \leq b_\phi < \infty$ , we have

$$\begin{aligned} &\left| \sum_{U'_n(x,y)} \phi\left(\frac{i}{k_1}, \frac{j}{k_1}\right) K^* \left( \frac{i}{k_1}, \frac{j}{k_1} \right) L^* \left( \frac{nd'_{ij}}{k_1} \right) \frac{1}{k_1^2} \right. \\ &\quad \left. - \sum_{\tilde{U}'_n(x,y)} \phi\left(\frac{i}{k_1}, \frac{j}{k_1}\right) K^* \left( \frac{i}{k_1}, \frac{j}{k_1} \right) L^* \left( \frac{n\tilde{d}'_{ij}}{k_1} \right) \frac{1}{k_1^2} \right| \\ &\leq \frac{1}{k_1^2} \left| \sum_{U'_n(x,y)} \phi\left(\frac{i}{k_1}, \frac{j}{k_1}\right) K^* \left( \frac{i}{k_1}, \frac{j}{k_1} \right) L^* \left( \frac{n\tilde{d}'_{ij}}{k_1} \right) \right. \\ &\quad \left. - \sum_{\tilde{U}'_n(x,y)} \phi\left(\frac{i}{k_1}, \frac{j}{k_1}\right) K^* \left( \frac{i}{k_1}, \frac{j}{k_1} \right) L^* \left( \frac{n\tilde{d}'_{ij}}{k_1} \right) \right| + \\ &\quad O\left(\frac{|d'_{ij} - \tilde{d}'_{ij}|}{k_1/n}\right) \end{aligned} \tag{S.17}$$



$$\begin{aligned}
&\leq b_\phi \|K\|_\infty \|L\|_\infty \left| \frac{1}{k_1^2} \sum_{U'_n(x,y) \Delta \tilde{U}'_n(x,y)} 1 \right| + O\left(\frac{|d'_{ij} - \tilde{d}'_{ij}|}{k_1/n}\right) \\
&= O(\delta_n) = o(1), \text{ a.s.}
\end{aligned}$$

where  $\delta_n$  denotes the acute angle between  $(\hat{b}(x,y), \hat{c}(x,y))$  and its asymptotic direction and  $U'_n(x,y) \Delta \tilde{U}'_n(x,y) = (U'_n(x,y) \setminus \tilde{U}'_n(x,y)) \cup (\tilde{U}'_n(x,y) \setminus U'_n(x,y))$ . In the first inequality of (S.17), we have used the Lipschitz-1 continuity of  $L^*$ . In the last equation, Lemma 1 has been applied. Now, let

$$\begin{aligned}
\tilde{b}_{i,j}(x,y) &= \left[ \tilde{B}_1(x,y) + \tilde{B}_2(x,y) \frac{i}{n} + \tilde{B}_3(x,y) \frac{j}{n} \right] K^* \left( \frac{i}{k_1}, \frac{j}{k_1} \right) L^*(n\tilde{d}'_{ij}/k_1), \\
\tilde{B}_1(x,y) &= \tilde{t}_{20}(x,y)\tilde{t}_{02}(x,y) - \tilde{t}_{11}(x,y)\tilde{t}_{11}(x,y), \\
\tilde{B}_2(x,y) &= \tilde{t}_{01}(x,y)\tilde{t}_{11}(x,y) - \tilde{t}_{10}(x,y)\tilde{t}_{02}(x,y), \\
\tilde{B}_3(x,y) &= \tilde{t}_{10}(x,y)\tilde{t}_{11}(x,y) - \tilde{t}_{01}(x,y)\tilde{t}_{20}(x,y), \\
\tilde{t}_{s_1,s_2}(x,y) &= \sum_{\tilde{U}'_n(x,y)} (i/n)^{s_1} (j/n)^{s_2} K^* \left( \frac{i}{k_1}, \frac{j}{k_1} \right) L^*(n\tilde{d}'_{ij}/k_1).
\end{aligned}$$

Then, by using similar arguments to those in (S.17), we can check that

$$I_1(x,y) = \frac{\sum_{\tilde{U}'_n(x,y)} \tilde{b}_{ij}(x,y) H\{f\}(x_i, y_j)}{\sum_{\tilde{U}'_n(x,y)} \tilde{b}_{ij}(x,y)} + O(\delta_n), \text{ a.s.} \quad (\text{S.18})$$

Also,

$$\begin{aligned}
I_2(x,y) &= \sum_{U'_n(x,y)} \frac{b_{ij}(x,y) \frac{n^4}{k_1^8}}{\frac{n^4}{k_1^{10}} \sum_{U'_n(x,y)} b_{ij}(x,y)} \frac{1}{k_1^2} \varepsilon_{ij} \\
&= \sum_{U'_n(x,y)} \frac{\frac{n^4}{k_1^8} \tilde{b}_{ij}(x,y) + O(\delta_n)}{\frac{n^4}{k_1^{10}} \sum_{\tilde{U}'_n(x,y)} \tilde{b}_{ij}(x,y) + O(\delta_n)} \frac{1}{k_1^2} \varepsilon_{ij} \\
&= \sum_{U'_n(x,y)} \left( \frac{\frac{n^4}{k_1^8} \tilde{b}_{ij}(x,y)}{\frac{n^4}{k_1^{10}} \sum_{\tilde{U}'_n(x,y)} \tilde{b}_{ij}(x,y)} + O(\delta_n) \right) \frac{1}{k_1^2} \varepsilon_{ij} \\
&= \sum_{U'_n(x,y)} \frac{\tilde{b}_{ij}(x,y)}{\sum_{\tilde{U}'_n(x,y)} \tilde{b}_{ij}(x,y)} \varepsilon_{ij} + \frac{1}{k_1^2} \sum_{U'_n(x,y)} O(\delta_n) \varepsilon_{ij} \\
&= O\left(\frac{\log(n)}{k_1}\right) + O(\delta_n), \text{ a.s.} \quad (\text{S.19})
\end{aligned}$$

In the second equation of (S.19), we have used (S.17) and the results that  $\tilde{B}_1(x,y) = O(k_1^8/n^4)$ ,  $\tilde{B}_2(x,y) = O(k_1^7/n^3)$ ,  $\tilde{B}_3(x,y) = O(k_1^7/n^3)$ , and  $\tilde{t}_{s_1,s_2}(x,y) = O\left(\frac{k_1^{s_1+s_2+2}}{n^{s_1+s_2}}\right)$ , for  $s_1, s_2 = 0, 1$ . The fifth equation is a direct conclusion of Proposition 2 in Qiu (2009), since  $\tilde{b}_{ij}(x,y)$  is deterministic. Now, for any given point  $(x,y)$  such that  $d_E((x,y), S) >$

$k_1/n$ ,  $O'_n(x, y)$  does not contain any step edge. By (S.9) and (S.13), we have

$$\begin{aligned}
& \frac{\sum_{\tilde{U}'_n(x,y)} \tilde{b}_{ij}(x, y) H\{f\}(x_i, y_j)}{\sum_{\tilde{U}'_n(x,y)} \tilde{b}_{ij}(x, y)} \\
&= \frac{\sum_{\tilde{U}'_n(x,y)} \tilde{b}_{ij}(x, y) (f(x + i/n, y + j/n) + O(R_n/n))}{\sum_{\tilde{U}'_n(x,y)} \tilde{b}_{ij}(x, y)} \\
&= \frac{\tilde{B}_1(x, y)}{|\tilde{\Delta}|} \sum_{\tilde{U}'_n(x,y)} (f(x, y) + O(k_1/n)O(R_n/n)) K^* \left( \frac{i}{k_1}, \frac{j}{k_1} \right) L^*(n\tilde{d}_{ij}/k_1) \\
&+ \frac{\tilde{B}_2(x, y)}{|\tilde{\Delta}|} \sum_{\tilde{U}'_n(x,y)} (f(x, y) + O(k_1/n) + O(R_n/n)) \frac{i}{n} K^* \left( \frac{i}{k_1}, \frac{j}{k_1} \right) L^*(n\tilde{d}_{ij}/k_1) \\
&+ \frac{\tilde{B}_3(x, y)}{|\tilde{\Delta}|} \sum_{\tilde{U}'_n(x,y)} (f(x, y) + O(k_1/n) + O(R_n/n)) \frac{j}{n} K^* \left( \frac{i}{k_1}, \frac{j}{k_1} \right) L^*(n\tilde{d}_{ij}/k_1) \\
&= f(x, y) + O(k_1/n) + O(R_n/n),
\end{aligned} \tag{S.20}$$

where  $|\tilde{\Delta}| = \tilde{t}_{00}(x, y)\tilde{t}_{20}(x, y)\tilde{t}_{02}(x, y) + 2\tilde{t}_{10}(x, y)\tilde{t}_{01}(x, y)\tilde{t}_{11}(x, y) - \tilde{t}_{01}(x, y)^2\tilde{t}_{20}(x, y) - \tilde{t}_{11}(x, y)^2\tilde{t}_{00}(x, y) - \tilde{t}_{10}(x, y)^2\tilde{t}_{02}(x, y)$ . In the second equation of (S.20), we have used (S.13) and the fact  $f$  has uniformly bounded directional derivatives. In the last equation, we have used the result that  $|\tilde{\Delta}| = \tilde{B}_1(x, y)\tilde{t}_{00}(x, y) + \tilde{B}_2(x, y)\tilde{t}_{10}(x, y) + \tilde{B}_3(x, y)\tilde{t}_{01}(x, y)$  and that  $\tilde{B}_1(x, y) = O(k_1^8/n^4)$ ,  $\tilde{B}_2(x, y) = O(k_1^7/n^3)$ ,  $\tilde{B}_3(x, y) = O(k_1^7/n^3)$ ,  $|\tilde{\Delta}| = O(k_1^{10}/n^4)$ ,  $\tilde{t}_{s_1, s_2}(x, y) = O\left(\frac{k_1^{s_1+s_2+2}}{n^{s_1+s_2}}\right)$ , for  $s_1, s_2 = 0, 1$ . All these results can be proved similarly to the result (23) in Proposition 2 of Qiu (2009). After combining (S.16), (S.18), (S.19) and (S.20), we have

$$\hat{a}_+(x, y) = f(x, y) + O(k_1/n) + O(R_n/n) + O\left(\frac{\log(n)}{k_1}\right) + O(\delta_n), \text{ a.s.} \tag{S.21}$$

Similarly, we have

$$\hat{a}_-(x, y) = f(x, y) + O(k_1/n) + O(R_n/n) + O\left(\frac{\log(n)}{k_1}\right) + O(\delta_n), \text{ a.s.} \tag{S.22}$$

From the proof of (S.5) and (S.6) in Lemma 1, we know that

$$\delta_n = O(R_n/k_1) + O(k_1/n) + O\left(\frac{n \log(n)}{k_1^2}\right), \text{ a.s.}$$

Thus,

$$\hat{a}_+(x, y) - \hat{a}_-(x, y) = O(R_n/k_1) + O(k_1/n) + O\left(\frac{n \log(n)}{k_1^2}\right), \text{ a.s.} \tag{S.23}$$

Also, by using similar arguments to those in (S.17) and the fact that  $\tilde{b}_{ij}(x, y) = O(k_1^{16}/n^8)$ , we have

$$\begin{aligned}
\frac{\sum_{U'_n(x,y)} b_{ij}^2(x,y)}{[\sum_{U'_n(x,y)} b_{ij}(x,y)]^2} &= \frac{\frac{k_1^{18}}{n^8} \frac{n^8}{k_1^{18}} \sum_{U'_n(x,y)} b_{ij}^2(x,y)}{\left[ \frac{k_1^{10}}{n^4} \frac{n^4}{k_1^{10}} \sum_{U'_n(x,y)} b_{ij}(x,y) \right]^2} \\
&= \frac{\frac{k_1^{18}}{n^8} \left( \frac{n^8}{k_1^{18}} \sum_{\tilde{U}'_n(x,y)} \tilde{b}_{ij}^2(x,y) + O(\delta_n) \right)}{\left[ \frac{k_1^{10}}{n^4} \left( \frac{n^4}{k_1^{10}} \sum_{\tilde{U}'_n(x,y)} \tilde{b}_{ij}(x,y) + O(\delta_n) \right) \right]^2} \\
&= \frac{1}{k_1^2} \frac{\frac{n^8}{k_1^{18}} \sum_{\tilde{U}'_n(x,y)} \tilde{b}_{ij}^2(x,y) + O(\delta_n)}{\left[ \frac{n^4}{k_1^{10}} \sum_{\tilde{U}'_n(x,y)} \tilde{b}_{ij}(x,y) + O(\delta_n) \right]^2} \\
&= \frac{1}{k_1^2} \left\{ \frac{\frac{n^8}{k_1^{18}} \sum_{\tilde{U}'_n(x,y)} \tilde{b}_{ij}^2(x,y)}{\left[ \frac{n^4}{k_1^{10}} \sum_{\tilde{U}'_n(x,y)} \tilde{b}_{ij}(x,y) \right]^2} + O(\delta_n) \right\}, \text{ a.s.}
\end{aligned}$$

Then, it follows that

$$\sqrt{\frac{\sum_{U'_n(x,y)} b_{ij}^2(x,y)}{[\sum_{U'_n(x,y)} b_{ij}(x,y)]^2} + \frac{\sum_{V'_n(x,y)} b_{ij}^2(x,y)}{[\sum_{V'_n(x,y)} b_{ij}(x,y)]^2}} = O\left(\frac{1}{k_1}\right), \text{ a.s.} \quad (\text{S.24})$$

Hence, by (S.23) and (S.24), we have

$$\frac{M_n^{(1)}(x,y)}{u_n} = O(R_n/u_n) + O\left(\frac{k_1^2}{u_n n}\right) + O\left(\frac{n \log(n)}{k_1 u_n}\right), \text{ a.s.} \quad (\text{S.25})$$

Now, consider any given nonsingular point  $(x, y)$  on a step edge. Then, the related step edge has a unique tangent line at  $(x, y)$ . Also, without loss of generality, we can assume that the step edge is a straight line in  $O'_n(x, y)$ . Suppose the step edge separates  $O'_n(x, y)$  into two halves, denoted by  $O'_{n,1}(x, y)$  and  $O'_{n,2}(x, y)$ , respectively. Then, it follows from (S.7) in Lemma 1 that  $\tilde{U}'_n(x, y) = O'_{n,1}(x, y)$ . By the same arguments as those in (S.20), we have

$$\frac{\sum_{\tilde{U}'_n(x,y)} \tilde{b}_{ij}(x,y) H\{f\}(x_i, y_j)}{\sum_{\tilde{U}'_n(x,y)} \tilde{b}_{ij}(x,y)} = f_+(x, y) + O(k_1/n) + O(R_n/n),$$

where  $f_+(x, y)$  denotes the limit of  $f(u, v)$  as  $(u, v)$  approaching  $(x, y)$  from  $\tilde{U}'_n(x, y)$ . Similar to (S.21) and (S.22), we have

$$\hat{a}_+(x, y) = f_+(x, y) + O(R_n/k_1) + O(k_1/n) + O\left(\frac{n \log(n)}{k_1^2}\right), \text{ a.s.}$$

$$\hat{a}_-(x, y) = f_-(x, y) + O(R_n/k_1) + O(k_1/n) + O\left(\frac{n \log(n)}{k_1^2}\right), \text{ a.s.}$$

Hence,

$$\frac{M_n^{(1)}(x,y)}{u_n} = O\left(\frac{k_1(f_+(x,y) - f_-(x,y))}{u_n}\right) + O\left(\frac{R_n}{u_n}\right) + O\left(\frac{k_1^2}{u_n n}\right) + O\left(\frac{n \log(n)}{k_1 u_n}\right), \text{ a.s.} \quad (\text{S.26})$$

where  $f_-(x, y)$  is defined similarly to  $f_+(x, y)$ . It follows from (S.25) and (S.26) that the proposed step edge detection procedure (6) could detect all points in  $S \cap \Omega_{k_1, n} \cap \bar{J}_{S, k_1, n}$ , and all points whose Euclidean distances to  $S$  are greater than  $k_1/n$  would not be detected. So, when  $n$  is sufficiently large,  $S \cap \Omega_{k_1, n} \cap \bar{J}_{S, k_1, n}$  is included in  $\hat{S}_n$ , and  $\hat{S}_n$  is included in the band of  $S$  with width  $k_1/n$ . Thus, the result (i) in Theorem 3.1 is proved. For roof/valley edge detection, results parallel to Lemma 1, (S.25) and (S.26) can be derived in a similar way. Therefore, the result (ii) in Theorem 3.1 is also valid.

### Proof Of Theorem 3.2

For a point  $(x, y) \in \Omega_{k, n} \setminus (S \cup RV)$ , by Theorem 3.1, we know that, when  $n$  is large enough, there would be no detected step or roof/valley edge points in  $O_n(x, y)$ . Therefore,  $\hat{f}(x, y)$  is defined by (11) in such cases, and

$$\begin{aligned}
\mathbb{E}(\hat{f}(x, y)) &= \frac{\sum_{i^2+j^2 \leq k^2} w_{ij}(x, y) H\{f\}(x + i/n, y + j/n)}{\sum_{i^2+j^2 \leq k^2} w_{ij}(x, y)} \\
&= \frac{\sum_{i^2+j^2 \leq k^2} w_{ij}(x, y) [f(x + i/n, y + j/n) + O(R_n/n)]}{\sum_{i^2+j^2 \leq k^2} w_{ij}(x, y)} \\
&= \frac{\sum_{i^2+j^2 \leq k^2} w_{ij}(x, y) [f(x, y) + O(k/n) + O(R_n/n)]}{\sum_{i^2+j^2 \leq k^2} w_{ij}(x, y)} \\
&= f(x, y) + O(k/n) + O(R_n/n). \tag{S.27}
\end{aligned}$$

In the second equation of (S.27), the result (S.9) has been used. In the third equation, we have used the property that  $f$  has continuous first-order derivatives in  $O_n(x, y)$ . Therefore, for any  $(x_i, y_j) \in O_n(x, y)$ , there is a constant  $C_1 > 0$  such that  $|f(x_i, y_j) - f(x, y)| \leq C_1 k/n$ . On the other hand, by similar results to (S.10) and by the fact that  $r_{s_1 s_2} = O(k^{s_1+s_2+2}/n^{s_1+s_2})$ , for  $s_1, s_2 = 0, 1, 2$ , we have

$$\begin{aligned}
&\hat{f}(x, y) - \mathbb{E}(\hat{f}(x, y)) \tag{S.28} \\
&= \frac{\sum_{i^2+j^2 \leq k^2} w_{ij}(x, y) \varepsilon_{ij}}{\sum_{i^2+j^2 \leq k^2} w_{ij}(x, y)} \\
&= \frac{A_1(x, y) \sum_{i^2+j^2 \leq k^2} \varepsilon_{ij} K\left(\frac{i}{k}, \frac{j}{k}\right) + A_2(x, y) \sum_{i^2+j^2 \leq k^2} \varepsilon_{ij} (i/n) K\left(\frac{i}{k}, \frac{j}{k}\right)}{A_1(x, y)r_{00} + A_2(x, y)r_{10} + A_3(x, y)r_{01}} \\
&+ \frac{A_3(x, y) \sum_{i^2+j^2 \leq k^2} \varepsilon_{ij} (j/n) K\left(\frac{i}{k}, \frac{j}{k}\right)}{A_1(x, y)r_{00} + A_2(x, y)r_{10} + A_3(x, y)r_{01}} \\
&= O\left(\frac{\log(n)}{k}\right), \text{ a.s.}
\end{aligned}$$

In the last equation, we have used (S.10) and the facts that  $A_1(x, y) = r_{20}(x, y)r_{02}(x, y) - r_{11}(x, y)r_{11}(x, y) = O(k^8/n^4)$ ,  $A_2(x, y) = O(k^7/n^3)$ , and  $A_3(x, y) = O(k^7/n^3)$ . Then, the result (i) of the theorem follows from (S.27) and (S.28).

Now, let us consider a point  $(x, y) \in S \setminus J_S$ . In such cases, from Theorem 3.1, we know that all design points in  $S \cap O_n(x, y)$  would be detected as step edge points by the procedure (6) and all design points outside  $S_{k_1, n}(x, y) = S_{k_1, n} \cap O_n(x, y)$  would not be detected. Because  $(x, y)$  is not a singular point,  $S$  has a tangent line at  $(x, y)$ . Without

loss of generality, we assume that  $S$  is a straight line with slope  $\gamma \neq \infty$ . Then, all detected step edge points in  $O_n(x, y)$  (i.e.,  $\{(w_l, v_l), l = 1, 2, \dots, m\}$ ) have the expression

$$v_l - y = \gamma(w_l - x) + O(k_1/n), \text{ a.s., for } l = 1, 2, \dots, m. \quad (\text{S.29})$$

So, by the results (B.1) and (B.2) in Qiu (1998), it is easy to check that  $\sigma_{wv} = \gamma\sigma_{ww} + O(k_1/n)$ ,  $\sigma_{vv} = \gamma^2\sigma_{ww} + O(k_1/n)$ , and the slope of the fitted PC line is  $\sigma_{wv}/(\sigma_{ww} + \lambda_1) = \gamma + O(k_1/n)$ , a.s.. By (S.29), we also know that  $(\bar{w}, \bar{v})$  converges to  $(x, y)$  almost surely with the rate  $O(k_1/n)$ . Let  $\tilde{U}_n(x, y)$  be the part of  $O_n(x, y)$  that is separated by  $S$  and contains  $(x, y)$ , then  $U_n(x, y) \setminus S_{k_1, n} = \tilde{U}_n(x, y) \setminus S_{k_1, n}$  since the fitted PC line would be contained in  $S_{k_1, n}$  when  $n$  is sufficiently large. And, without loss of generality, we can assume that  $f(x, y)$  equals the limit of  $f(u, v)$  as  $(u, v)$  approaches  $(x, y)$  from  $\tilde{U}_n(x, y)$ . Let  $\tilde{d}_{ij}$  be the Euclidean distance from  $(x_i, y_j)$  to  $S$ . Then, by (9), we have

$$\begin{aligned} & \frac{\sum_{U_n(x, y)} \tilde{w}_{ij}(x, y) H\{f\}(x+i/n, y+j/n)}{\sum_{U_n(x, y)} \tilde{w}_{ij}(x, y)} \quad (\text{S.30}) \\ &= \frac{\sum_{\tilde{U}_n(x, y)} \tilde{w}_{ij}(x, y) H\{f\}(x+i/n, y+j/n)}{\sum_{\tilde{U}_n(x, y)} \tilde{w}_{ij}(x, y)} + O\left(\frac{k_1}{k}\right) \\ &= \frac{\sum_{\tilde{U}_n(x, y)} K\left(\frac{i}{k}, \frac{j}{k}\right) L\left(\frac{\tilde{d}_{ij}}{k/n}\right) \int h(u, v; x_i, y_j) f\left(x + \frac{i}{n} - u, y + \frac{j}{n} - v\right) dudv}{\sum_{\tilde{U}_n(x, y)} K\left(\frac{i}{k}, \frac{j}{k}\right) L\left(\frac{\tilde{d}_{ij}}{k/n}\right)} + O\left(\frac{k_1}{k}\right) \\ &= f(x, y) - C(x, y) \frac{\sum_{\tilde{U}_n(x, y)} K\left(\frac{i}{k}, \frac{j}{k}\right) L\left(\frac{\tilde{d}_{ij}}{k/n}\right) \int_{u > i/r_n(x, y)} \tilde{h}(u, v; x_i, y_j) dudv}{\sum_{\tilde{U}_n(x, y)} K\left(\frac{i}{k}, \frac{j}{k}\right) L\left(\frac{\tilde{d}_{ij}}{k/n}\right)} \\ &\quad + O\left(\frac{k}{n}\right) + O\left(\frac{r_n(x, y)}{n}\right) + O\left(\frac{k_1}{k}\right) \\ &= f(x, y) - C(x, y) \frac{\int_0^1 \int_{-1}^1 K(s, t) dt L(s) \int_{u > s \frac{k}{r_n(x, y)}} \tilde{h}(u, v; x, y) dudv ds}{\int_0^1 \int_{-1}^1 K(s, t) dt L(s) ds} \\ &\quad + O\left(\frac{k_1}{k}\right) + O\left(\frac{k}{n}\right). \end{aligned}$$

In the first equation of (S.30), we have used the result that

$$\mathcal{T}(U_n(x, y) \cap S_{k_1, n}(x, y)) / \mathcal{T}(O_n(x, y)) = O(k_1/k), \quad (\text{S.31})$$

where  $\mathcal{T}(O_n(x, y))$  denotes the area of  $O_n(x, y)$ , the condition that  $H\{f\}(x_i, y_j)$  is uniformly bounded, and the following fact:

if  $\frac{B_n}{A_n} = O(\alpha_n)$ ,  $\frac{D_n}{C_n} = O(\alpha_n)$ ,  $\frac{A_n}{C_n} \rightarrow \Gamma$ , and  $\alpha_n \rightarrow 0$ , then  $\frac{A_n + B_n}{C_n + D_n} = \frac{A_n}{C_n} + O(\alpha_n)$ ,

where  $\{A_n\}$ ,  $\{B_n\}$ ,  $\{C_n\}$  and  $\{D_n\}$  are sequences of numbers, and  $\Gamma$  is a constant. Now, by similar arguments to those in (S.19), we can check that

$$\begin{aligned} & \frac{\sum_{U_n(x, y)} K\left(\frac{i}{k}, \frac{j}{k}\right) L\left(\frac{d_{ij}}{k/n + d(x, y)}\right) \varepsilon_{ij}}{\sum_{U_n(x, y)} K\left(\frac{i}{k}, \frac{j}{k}\right) L\left(\frac{d_{ij}}{k/n + d(x, y)}\right)} \quad (\text{S.32}) \\ &= \frac{\sum_{\tilde{U}_n(x, y) \setminus S_{k_1, n}} K\left(\frac{i}{k}, \frac{j}{k}\right) L\left(\frac{d_{ij}}{k/n + d(x, y)}\right) \varepsilon_{ij}}{\sum_{U_n(x, y)} K\left(\frac{i}{k}, \frac{j}{k}\right) L\left(\frac{d_{ij}}{k/n + d(x, y)}\right)} + \frac{\sum_{U_n(x, y) \cap S_{k_1, n}} K\left(\frac{i}{k}, \frac{j}{k}\right) L\left(\frac{d_{ij}}{k/n + d(x, y)}\right) \varepsilon_{ij}}{\sum_{U_n(x, y)} K\left(\frac{i}{k}, \frac{j}{k}\right) L\left(\frac{d_{ij}}{k/n + d(x, y)}\right)} \end{aligned}$$

$$\begin{aligned}
&= \frac{\sum_{\tilde{U}_n(x,y) \setminus S_{k_1,n}} K\left(\frac{i}{k}, \frac{j}{k}\right) L\left(\frac{\tilde{d}_{ij}}{k/n}\right) \varepsilon_{ij}}{\sum_{U_n(x,y)} K\left(\frac{i}{k}, \frac{j}{k}\right) L\left(\frac{d_{ij}}{k/n+d(x,y)}\right)} + \frac{\sum_{\tilde{U}_n(x,y) \setminus S_{k_1,n}} K\left(\frac{i}{k}, \frac{j}{k}\right) O\left(\frac{k_1}{k}\right) \varepsilon_{ij}}{\sum_{U_n(x,y)} K\left(\frac{i}{k}, \frac{j}{k}\right) L\left(\frac{d_{ij}}{k/n+d(x,y)}\right)} + \\
&\quad \frac{\sum_{U_n(x,y) \cap S_{k_1,n}} K\left(\frac{i}{k}, \frac{j}{k}\right) L\left(\frac{d_{ij}}{k/n+d(x,y)}\right) \varepsilon_{ij}}{\sum_{U_n(x,y)} K\left(\frac{i}{k}, \frac{j}{k}\right) L\left(\frac{d_{ij}}{k/n+d(x,y)}\right)} \\
&= \frac{\sum_{\tilde{U}_n(x,y) \setminus S_{k_1,n}} K\left(\frac{i}{k}, \frac{j}{k}\right) L\left(\frac{\tilde{d}_{ij}}{k/n}\right) \varepsilon_{ij}}{\sum_{\tilde{U}_n(x,y) \setminus S_{k_1,n}} K\left(\frac{i}{k}, \frac{j}{k}\right) L\left(\frac{\tilde{d}_{ij}}{k/n}\right) + k^2 O\left(\frac{k_1}{k}\right) + \sum_{U_n(x,y) \cap S_{k_1,n}} K\left(\frac{i}{k}, \frac{j}{k}\right) L\left(\frac{d_{ij}}{k/n+d(x,y)}\right)} \\
&+ \frac{\sum_{\tilde{U}_n(x,y) \setminus S_{k_1,n}} K\left(\frac{i}{k}, \frac{j}{k}\right) O\left(\frac{k_1}{k}\right) \varepsilon_{ij}}{\sum_{\tilde{U}_n(x,y) \setminus S_{k_1,n}} K\left(\frac{i}{k}, \frac{j}{k}\right) L\left(\frac{\tilde{d}_{ij}}{k/n}\right) + k^2 O\left(\frac{k_1}{k}\right) + \sum_{U_n(x,y) \cap S_{k_1,n}} K\left(\frac{i}{k}, \frac{j}{k}\right) L\left(\frac{d_{ij}}{k/n+d(x,y)}\right)} \\
&+ \frac{\sum_{U_n(x,y) \cap S_{k_1,n}} K\left(\frac{i}{k}, \frac{j}{k}\right) L\left(\frac{d_{ij}}{k/n+d(x,y)}\right) \varepsilon_{ij}}{\sum_{\tilde{U}_n(x,y) \setminus S_{k_1,n}} K\left(\frac{i}{k}, \frac{j}{k}\right) L\left(\frac{\tilde{d}_{ij}}{k/n}\right) + k^2 O\left(\frac{k_1}{k}\right) + \sum_{U_n(x,y) \cap S_{k_1,n}} K\left(\frac{i}{k}, \frac{j}{k}\right) L\left(\frac{d_{ij}}{k/n+d(x,y)}\right)} \\
&= O\left(\frac{\log(n)}{k}\right) + O\left(\frac{k_1}{k}\right). \text{ a.s.}
\end{aligned}$$

In the first equation of (S.32), we have used the fact that  $U_n(x, y) \setminus S_{k_1, n} = \tilde{U}_n(x, y) \setminus S_{k_1, n}$ . In the second and third equations, the Lipschitz-1 continuity of  $L$  has been used. In the fourth equation, we have used the fact that

$$\frac{1}{k^2} \sum_{U_n(x,y) \cap S_{k_1,n}} K\left(\frac{i}{k}, \frac{j}{k}\right) L\left(\frac{d_{ij}}{k/n+d(x,y)}\right) = O\left(\frac{k_1}{k}\right),$$

which follows from (S.31), the result that

$$\frac{1}{k^2} \sum_{\tilde{U}_n(x,y) \setminus S_{k_1,n}} K\left(\frac{i}{k}, \frac{j}{k}\right) L\left(\frac{\tilde{d}_{ij}}{k/n}\right) \varepsilon_{ij} = O\left(\frac{\log(n)}{k}\right)$$

derived from Proposition 2 in Qiu (2009), and the obvious result that

$$\frac{1}{k^2} \sum_{\tilde{U}_n(x,y) \setminus S_{k_1,n}} K\left(\frac{i}{k}, \frac{j}{k}\right) L\left(\frac{\tilde{d}_{ij}}{k/n}\right) \rightarrow \int_0^\pi \int_0^1 r \tilde{K}(r) L(r \sin \varphi) d\varphi dr,$$

where  $\tilde{K}(r) = K(r \cos \varphi, r \sin \varphi)$ .

Finally, we consider the case when  $(x, y) \in RV \setminus J_{RV}$ . From the above arguments, we can check that (S.30) and (S.32) still hold after we replace the detected step edge points by the detected roof/valley edge points. Therefore, the results (ii) and (iii) of the theorem are valid.

### S.3 Some Simulation Results

In this part, we present two artificial numerical examples concerning the numerical performance of the proposed BID procedure (8)–(11). The kernel functions  $K^*$  and  $K$

used in (3), (S.1) and (12) are both chosen to be the truncated Gaussian density functions, i.e.,  $1/(2\pi - 3\pi \exp(-0.5)) [\exp(-(x^2 + y^2)/2) - \exp(-0.5)] I_{x^2+y^2 \leq 1}$ , the kernel functions  $L^*$  and  $L$  used in (4), (5), (S.2), (S.3) and (12) are both chosen to be  $1/1.194958 \exp(x^2/2) I_{0 \leq x \leq 1}$ , which is proportional to the reciprocal of the 1-D truncated Gaussian density function,  $w$  in (16) and  $\tilde{w}$  in (17) are both fixed at 0.5, and  $B$  in (16) and (17) is chosen to be 100. Degraded images are generated from model (2), in which the psf is chosen to be

$$h(u, v; x, y) = \frac{3}{\pi} \left( 1 - \frac{\sqrt{u^2 + v^2}}{r_n(x, y)/n} \right) I_{\sqrt{u^2 + v^2} \leq r_n(x, y)/n},$$

and the additive random errors  $\varepsilon_{ij}$  follow the distribution  $N(0, \sigma^2)$ . The above psf is circularly symmetric with the blurring extent  $r_n(x, y)$  which may depend on  $(x, y)$ . Let  $\rho_n(x, y) = r_n(x, y)/n$  denote the blurring-extent-to-sample-size ratio (BSR) at  $(x, y)$ . We first consider the following true image intensity functions:

$$f_1(x, y) = \begin{cases} 1 - (x - 0.5)^2 - (y - 0.5)^2, & \text{if } (x - 0.5)^2 + (y - 0.5)^2 \leq 0.25^2, \\ -(x - 0.5)^2 - (y - 0.5)^2, & \text{otherwise.} \end{cases}$$

It is shown in Figure S.1 by a 3-D plot, from which it can be seen that  $f_1$  has one

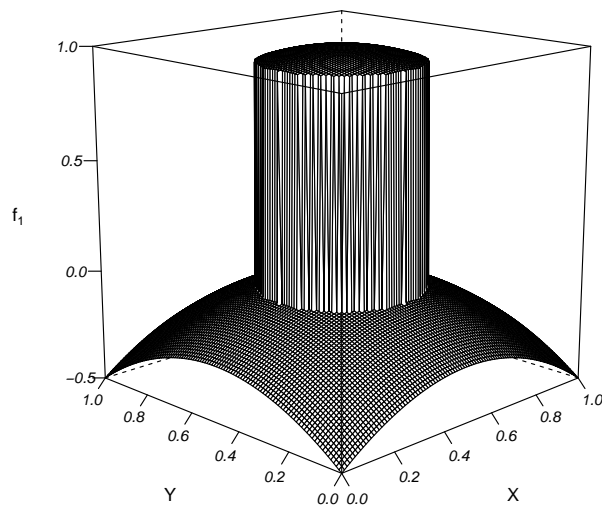


Figure S.1: A 3-D plot of  $f_1(x, y)$ .

circular step edge and it does not have any roof/valley edges. Figure S.2(a) shows the original true image of  $f_1$ , and Figure S.2(b) shows an observed image when  $\sigma = 0.1$ ,  $\rho_n^{(1)}(x, y) = 0.03(1 - (x - 0.5)^2 - (y - 0.5)^2) + 0.02$ , and  $n = 100$ . The detected step

edges are shown in Figure S.2(c). Finally, the deblurred image is displayed in Figure S.2(d). The parameters  $k_1$ ,  $u_n$ , and  $k$  are selected to be 8, 4.9 and 4, respectively, in this example. It can be seen from the figure that, in the deblurred image, the noise has been mostly removed and the spatial blur has also been significantly reduced, which confirms our theoretical justification discussed in the previous section.

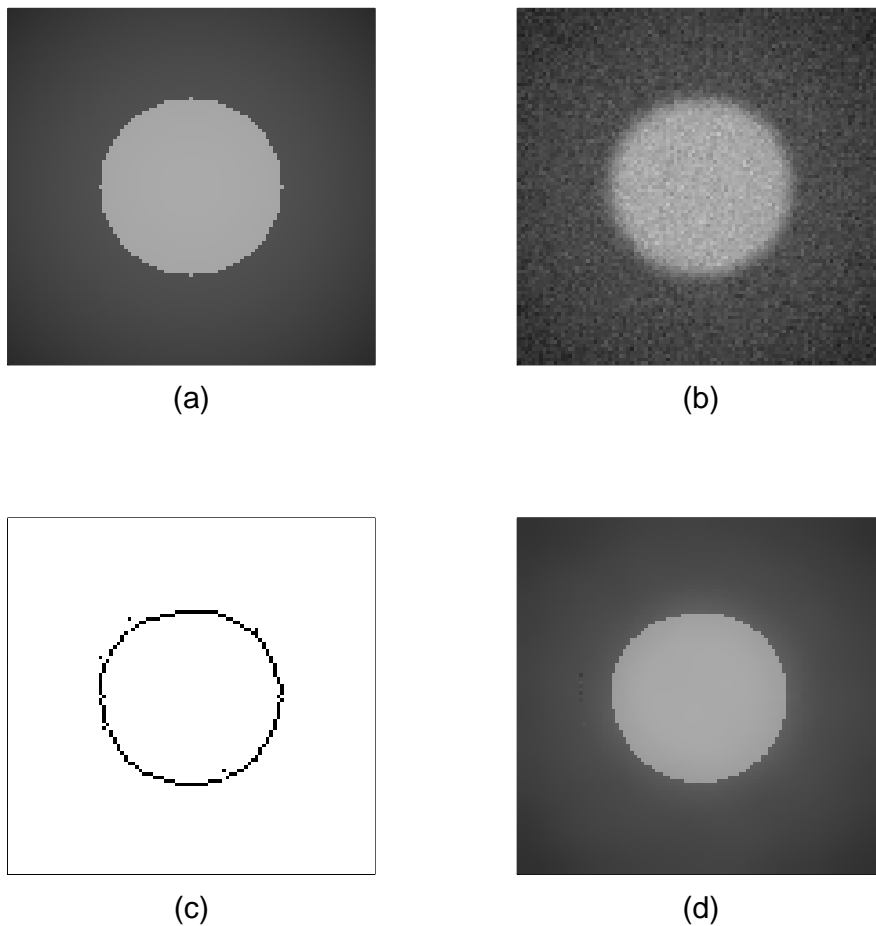


Figure S.2: (a): True image; (b): Observed image; (c): Detected step edges; (d): Deblurred image.

Next, the performance of our proposed method is measured quantitatively. We consider two BSR functions  $\rho_n^{(1)}(x, y) = 0.03(1 - (x - 0.5)^2 - (y - 0.5)^2) + 0.02$  and  $\rho_n^{(2)}(x, y) = 0.05x$ , two sample sizes  $n = 100$  and  $200$ , and three  $\sigma$  values  $0.05$ ,  $0.1$  and  $0.2$ . Simulation results based on 100 replications are presented in Table S.1. In the simulation, for each combination of  $\rho_n(x, y)$ ,  $n$ , and  $\sigma$ , the parameters  $(k_1, u_n)$  and  $k$  are chosen



sequentially by minimizing the averaged values of  $d_Q(\hat{S}_n, S; k_1, u_n)$  and  $\text{MSE}(\hat{f}, f) = \frac{1}{n^2} \sum_{i=1}^n \sum_{j=1}^n (\hat{f}(x_i, y_j) - f(x_i, y_j))^2$ , respectively. Such parameter values are called optimal ones hereafter. Parameters chosen by our proposed bootstrap procedures (16) and (17) are also presented in the table. From the table, it can be seen that (i)  $\text{MSE}(\hat{f}, f)$  increases as  $\sigma$  increases, and decreases as  $n$  increases, and (ii) parameters chosen via our proposed bootstrap procedure are quite close to their optimal ones, and this is true especially when the sample size gets large, with the optimal values of  $k_1$  and  $u_n$  slightly smaller than their values chosen by the bootstrap procedure.

Table S.1: Simulation results of the BID procedure (8)–(11) in the example of Figure S.2 based on 100 replications. In each entry, the first line presents the optimal values of  $k_1/n$ ,  $u_n$  and  $k/n$ , the second line presents their values chosen by the proposed bootstrap procedure with  $B = 100$ , the third line presents the value of  $d_Q(\hat{S}_n, S; k_1, u_n)$ , and the fourth line presents the value of  $\text{MSE}(\hat{f}, f)$ .

$n$	$\sigma = .05$	$\rho_n^{(1)}(x, y)$ $\sigma = .1$	$\sigma = .2$
	100	(0.07, 6.2, 0.04)	(0.08, 4.9, 0.04)
(0.08, 7.8, 0.02)		(0.10, 8.6, 0.03)	(0.12, 4.8, 0.08)
$1.07 \times 10^{-2}$		$1.37 \times 10^{-2}$	$1.62 \times 10^{-2}$
$5.44 \times 10^{-3}$		$6.23 \times 10^{-3}$	$8.44 \times 10^{-3}$
200	(0.06, 8.6, 0.04)	(0.08, 9.5, 0.035)	(0.105, 10.0, 0.035)
	(0.06, 8.5, 0.02)	(0.09, 9.8, 0.02)	(0.11, 10.2, 0.03)
	$0.785 \times 10^{-2}$	$0.980 \times 10^{-2}$	$1.12 \times 10^{-2}$
	$5.33 \times 10^{-3}$	$6.02 \times 10^{-3}$	$7.54 \times 10^{-3}$
$n$	$\sigma = .05$	$\rho_n^{(2)}(x, y)$ $\sigma = .1$	$\sigma = .2$
	100	(0.08, 13.1, 0.02)	(0.08, 6.5, 0.03)
(0.10, 16.1, 0.07)		(0.10, 8.0, 0.08)	(0.11, 5.7, 0.08)
$1.15 \times 10^{-2}$		$1.03 \times 10^{-2}$	$1.15 \times 10^{-2}$
$3.99 \times 10^{-3}$		$4.72 \times 10^{-3}$	$6.05 \times 10^{-3}$
200	(0.065, 19.5, 0.03)	(0.065, 9.6, 0.03)	(0.07, 5.9, 0.03)
	(0.065, 20.7, 0.03)	(0.075, 9.2, 0.055)	(0.08, 5.1, 0.06)
	$0.73 \times 10^{-2}$	$0.84 \times 10^{-2}$	$0.88 \times 10^{-2}$
	$3.32 \times 10^{-3}$	$3.56 \times 10^{-3}$	$4.14 \times 10^{-3}$

Next, we consider another example with the following true image intensity function:

$$f_2(x, y) = \begin{cases} 0, & \text{if } x \leq 0.5 \text{ and } y > 0.5 \\ 1, & \text{if } x > 0.5 \text{ and } y > 0.5 \\ 3, & \text{if } x > 0.5 \text{ and } y \leq 0.5 \\ -1, & \text{if } x \leq 0.25 \text{ and } y \leq 0.5 \\ 16(x - 0.25) - 1, & \text{if } 0.25 < x \leq 0.5 \text{ and } y \leq 0.5. \end{cases}$$

The surface of  $f_2$  is shown in Figure S.3(a), from which it can be seen that  $f_2$  has several step edge segments and two roof/valley edge segments at  $(x = 0.25, y \leq 0.5)$  and

( $x = 0.5, y \leq 0.5$ ). Figure S.3(b) shows a 3-D plot of an observed surface in the case when  $\rho_n^{(2)}(x, y) = 0.05x$ ,  $\sigma = 0.2$ , and  $n = 100$ . Figure S.3(c) shows the deblurred surface by our BID procedure, using the corresponding parameter values presented in Table S.2. The observed surface of  $f_2$  is then shown as an image in Figure S.3(d). The detected edge segments are shown in Figure S.3(e), in which step edges are shown in black and roof/valley edges are shown in gray. Finally, the deblurred image by our proposed BID procedure is shown in Figure S.3(f). From the figure, it can be seen that (i) spatial blur gets severer as  $x$  gets larger in the observed image, (ii) the pointwise noise and the spatial blur are well removed in the deblurred image by the BID procedure (8)–(11), (iii) both step edges and roof/valley edges have been detected successfully except at places around certain singular points (cf., Section 3 for their definition).

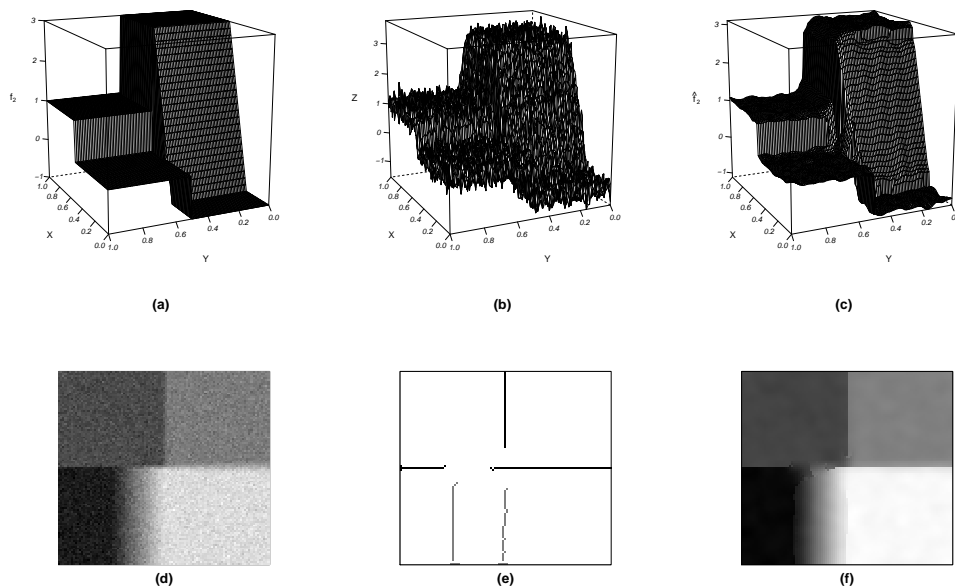


Figure S.3: (a)-(c): 3-D plots of the true surface, observed surface, and deblurred surface of  $f_2(x, y)$ ; (d)-(f): Observed image, detected step edge segments (black lines) and detected roof/valley edge segments (gray lines), and deblurred image.

Some numerical results in a similar setup to that of Table S.1 are presented in Table S.2. From the table, it can be seen that (i) values of  $d_Q(\hat{S}_n, S)$ ,  $d_Q(\widehat{RV}_n, RV)$  and  $\text{MSE}(\hat{f}, f)$  increase as the noisy level  $\sigma$  increases, and decrease as the sample size  $n$  increases, (ii) the value of the bandwidth  $k/n$  chosen by the bootstrap procedure (17) is close to its optimal value, and (iii) as the observed image gets noisier (i.e.,  $\sigma$  is larger), the bandwidths  $k_1$ ,  $k_2$ ,  $k$  and  $k^B$  should generally be chosen larger, which is intuitively reasonable because more observations should be used in local smoothing to remove noise in such cases.

Table S.2: Simulation results of the BID procedure (8)–(11) in the example of Figure S.3 based on 100 replications. In each entry, the first line presents the optimal values of  $k_1/n$  and  $u_n$ , the second line presents the  $d_Q$  value of the detected step edges, the third line presents the optimal values of  $k_2/n$  and  $v_n$ , the fourth line present the  $d_Q$  value of the detected roof/valley edges, the fifth line presents the values of  $k/n$  and  $k^B/n$ , and the sixth line presents the value of  $\text{MSE}(\hat{f}, f)$ .

$n$	$\rho_n^{(1)}(x, y)$		
	$\sigma = .1$	$\sigma = .2$	$\sigma = .3$
100	(0.13, 11.1)	(0.18, 13.1)	(0.18, 9.0)
	$5.085 \times 10^{-3}$	$8.103 \times 10^{-3}$	$9.591 \times 10^{-3}$
	(0.09, 4.3)	(0.10, 2.8)	(0.11, 2.9)
	$4.935 \times 10^{-3}$	$8.282 \times 10^{-3}$	$9.998 \times 10^{-3}$
	(0.04, 0.04)	(0.05, 0.06)	(0.05, 0.06)
	$9.199 \times 10^{-3}$	$11.21 \times 10^{-3}$	$13.01 \times 10^{-3}$
200	(0.11, 18.0)	(0.13, 10.7)	(0.17, 16.0)
	$3.124 \times 10^{-3}$	$4.357 \times 10^{-3}$	$4.546 \times 10^{-3}$
	(0.085, 7.8)	(0.105, 7.5)	(0.105, 5.0)
	$2.668 \times 10^{-3}$	$5.958 \times 10^{-3}$	$6.815 \times 10^{-3}$
	(0.045, 0.025)	(0.035, 0.035)	(0.05, 0.045)
	$9.181 \times 10^{-3}$	$9.349 \times 10^{-3}$	$10.53 \times 10^{-3}$
$n$	$\rho_n^{(2)}(x, y)$		
	$\sigma = .1$	$\sigma = .2$	$\sigma = .3$
100	(0.11, 15.2)	(0.12, 9.0)	(0.12, 6.1)
	$3.143 \times 10^{-3}$	$4.340 \times 10^{-3}$	$6.026 \times 10^{-3}$
	(0.10, 5.9)	(0.10, 3.0)	(0.10, 2.0)
	$3.581 \times 10^{-3}$	$6.815 \times 10^{-3}$	$9.193 \times 10^{-3}$
	(0.04, 0.04)	(0.05, 0.06)	(0.05, 0.08)
	$4.852 \times 10^{-3}$	$6.689 \times 10^{-3}$	$7.989 \times 10^{-3}$
200	(0.085, 23.0)	(0.115, 16.2)	(0.115, 10.9)
	$1.589 \times 10^{-3}$	$2.375 \times 10^{-3}$	$2.913 \times 10^{-3}$
	(0.095, 11.1)	(0.105, 8.0)	(0.11, 6.0)
	$1.713 \times 10^{-3}$	$3.453 \times 10^{-3}$	$4.234 \times 10^{-3}$
	(0.045, 0.045)	(0.05, 0.055)	(0.05, 0.055)
	$4.255 \times 10^{-3}$	$5.721 \times 10^{-3}$	$6.118 \times 10^{-3}$